Corrigendum to Earth Surf. Dynam., 11, 305–324, 2023
https://doi.org/10.5194/esurf-11-305-2023-corrigendum

Earth Surface Dynamics
Open Access

Corrigendum to "The story of a summit nucleus: hillslope boulders and their effect on erosional patterns and landscape morphology in the Chilean Coastal Cordillera" published in Earth Surf. Dynam., 11, 305–324, 2023

Emma Lodes[1,a], Dirk Scherler[1,2], Renee van Dongen[3], and Hella Wittmann[1]

[1]Earth Surface Geochemistry, GFZ German Research Centre for Geosciences, Telegrafenberg, 14473 Potsdam, Germany
[2]Institute of Geographical Sciences, Freie Universität Berlin, 12249 Berlin, Germany
[3]International Centre for Water Resources and Global Change, 56068 Koblenz, Germany
[a]now at: School of Earth and Space Exploration, Arizona State University, 85281 Tempe, Arizona, USA

Correspondence: Emma Lodes (elodes@asu.edu)

Published: 16 October 2024

This corrigendum includes a revised Eq. (1), revised versions of Figs. 3, 6 and 8, and revised values for Table 2.

We have found an error in the way we set up the model used to calculate denudation rates of boulders during two phases of exhumation based on ^{10}Be concentrations. In the published version of the model, we erroneously assumed that the sampled part of the exhuming boulder is at the top of the boulder, while the boulder is belowground and being exhumed. However, the sampled part should start out deeper within the boulder at the end of phase 1 and get closer to the surface as the boulder erodes and shrinks in size during phase 2. To illustrate this, we show an updated version of Fig. 3 below, where we added a red dot that indicates the position of the sample. As a result of this error, the amount of ^{10}Be accumulated during the first phase of our model, when the boulder remains below the surface, should be lower than initially assumed. In order to correct this, we revised Eq. (1), which has a newly added exponential term that reflects the depth correction:

$$N_{\text{modeled}} = \sum_i \frac{P_i(0)}{\lambda + \frac{\epsilon_s \rho}{\Lambda_i}} e^{-\left[\frac{t_2 \epsilon_b \rho}{\Lambda_i}\right]} e^{-t_2 \lambda} + \sum_i \frac{P_i(0)}{\lambda + \frac{\epsilon_b \rho}{\Lambda_i}} \left[1 - e^{-t_2\left(\lambda + \frac{\epsilon_b \rho}{\Lambda_i}\right)}\right]. \quad (1)$$

In the revised Eq. (1), N_{modeled} is the modeled ^{10}Be concentration (atoms g^{-1}); i indicates different terms for the production by spallation, fast muons, and negative muons; $P_i(0)$ represents the site-specific ^{10}Be surface production rates in atoms $g^{-1}\,yr^{-1}$ for the different production pathways; ϵ_s is the soil denudation rate; ϵ_b is the boulder denudation rate (cm yr^{-1}); λ is the ^{10}Be decay constant (4.9975×10^{-7}); Λ_i is the attenuation length scale (160 g cm^{-2} for spallation, 4320 g cm^{-2} for fast muons, and 1500 g cm^{-2} for negative muons; Braucher et al., 2011); ρ is the bedrock and boulder density, and here we use a value of 2.6 g cm^{-3} for all samples; z is the boulder protrusion height (cm); and t_2 is the exposure time of the boulder and the duration of phase 2, equal to the boulder protrusion divided by the difference in the two erosion rates, $t_2 = z/(\epsilon_s - \epsilon_b)$. Now, the depth within the boulder at the end of phase 1 (the soil erosion phase) corresponds to the amount that is eroded during phase 2 (the boulder erosion phase), i.e., the erosion rate of phase 2 times the duration of phase 2. Correcting this error does not change any interpretations or conclusions of the article, and the relative differences that we observed and reported are still valid. However, it does change the absolute boulder erosion rates by 30 %–50 %. In addition, we have corrected one of the average protrusion values, from Casa de Piedras, after incorporating two extra protrusion measurements.

Published by Copernicus Publications on behalf of the European Geosciences Union.

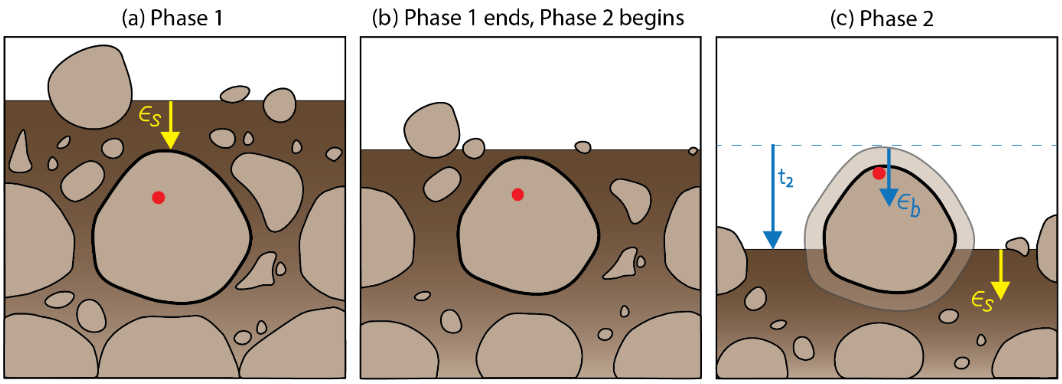

Figure 3. Schematic image showing the process of boulder exhumation where the red dot represents the final sampling point. **(a)** During phase 1, the boulder is buried and accumulates nuclides at a rate governed by the soil denudation rate, ϵ_s. **(b)** Phase 1 ends when the boulder breaches the soil surface, but the sampling point remains below the surface of the boulder. **(c)** During phase 2, the boulder itself is eroding at a rate of ϵ_b, and the surrounding soil continues to denude at a rate of ϵ_s. Phase 2 lasts for a time period t_2 that ends with our sampling, as the sampling point has reached the surface of the boulder.

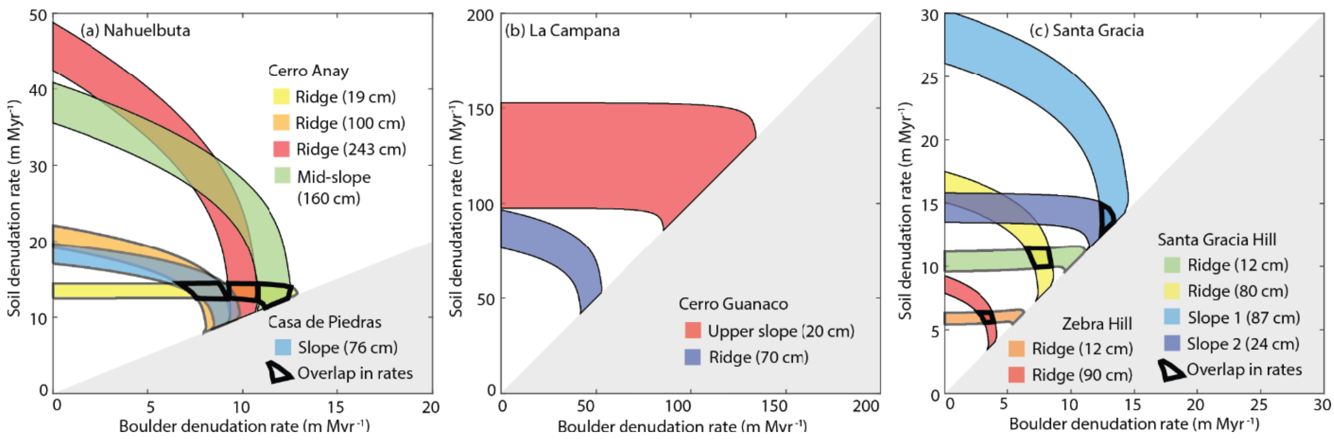

Figure 6. Range of best-fitting combinations of modeled soil and boulder denudation rates in **(a)** Nahuelbuta, **(b)** La Campana, and **(c)** Santa Gracia according to Eq. (1). Each color band corresponds to an amalgamated boulder sample, listed in the legend along with the average protrusion height of the boulders. Areas where best-fitting denudation rates overlap for samples from the same location are highlighted by a black outline. The gray areas are forbidden fields, as by assumption, boulder denudation rates have to be lower than soil denudation rates; otherwise, there would be no boulder protruding above the soil surface.

 https://doi.org/10.5194/esurf-11-305-2023

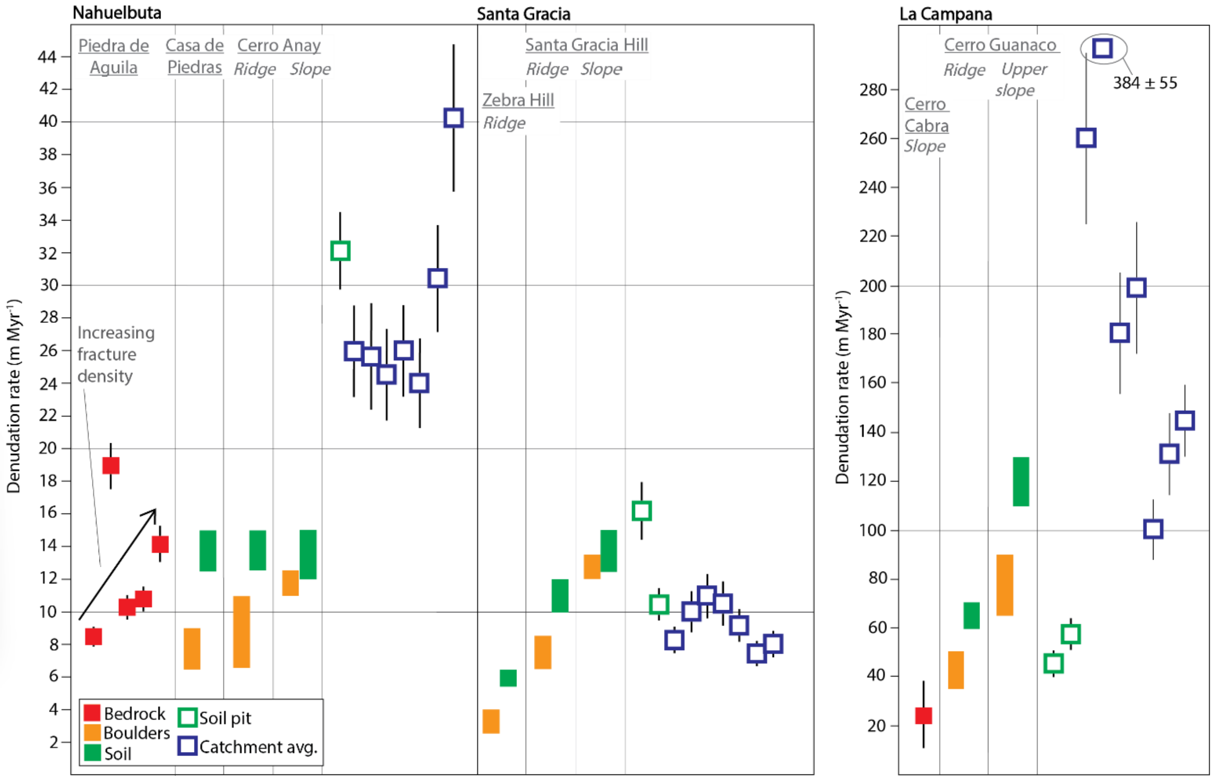

Figure 8. Overview of new and previously published denudation rates (data from this study are shown by solid symbols, and previously published data are shown by hollow symbols). Soil pit data are from Schaller et al. (2018), and catchment average data are from van Dongen et al. (2019). Catchment average denudation rates from various sediment grain sizes (from left to right for each field site: 0.5–1, 1–2, 2–4, 4–8, 8–16, 16–32, and 32–64 mm). Bedrock denudation rates are calculated using the CRONUS online calculator v2.3 (Balco et al., 2008). Boulder and soil denudation rates are estimated using our model and reflect the most plausible denudation rates as described in Sect. 5.1.2. Denudation rates for each location within a field site are separated by thin gray bars, and locations are labeled at the top of the chart. Samples that were not included in the model (one sample from Nahuelbuta and three samples from La Campana) are also not included here.

Table 2. Modeled denudation rates for soil and boulder samples using the first term of Eq. (1) and comparison of modeled and measured ^{10}Be concentrations for soil samples. Sample location abbreviations are described in the caption to Table 1.

Sample location	Soil sample ID	Best-fitting modeled soil denudation range rate (ϵ_s) (m Myr^{-1})	Corresp. modeled range of ^{10}Be conc. ($\times 10^5$) (atoms g^{-1}) for soil (N_m)	Measured ^{10}Be conc. $\pm 2\sigma$ ($\times 10^5$) (atoms g^{-1})	Boulder sample IDs	Best-fitting modeled boulder denudation rate range (ϵ_b) (m Myr^{-1})	Differential erosion rate (boulder vs. soil; m Myr^{-1})	Time needed for boulder exposure (Kyr)
Nahuelbuta								
CdP	NA5	12.5–15	4.34–5.15	2.32 ± 0.20	NA4	6.5–9	6	113
CA ridge	NA10	12.5–15	4.66–5.55	5.04 ± 0.36	NA7, NA8, NA9	6.5–11	5	200, 486, 38
CA slope	NA12	12–15	4.62–5.7	4.27 ± 0.32	NA11	11–12.5	1.75	914
La Campana								
CG ridge	LC12	60–70	0.637–0.737	0.88 ± 0.08	LC11	35–50	35	20
CG upper slope	LC14	110–130	0.335–0.395	0.63 ± 0.08	LC13	65–90	60	3
Santa Gracia								
SGH ridge	SG10	10–12	3.13–3.7	2.58 ± 0.22	SG8, SG9	6.5–8.5	3.5	229, 34
SGH slope 1	SG12	12.5–15	2.48–2.94	2.39 ± 0.18	SG11	12–13.5	1	870
SGH slope 2	SG23	12.5–15	2.47–2.94	2.10 ± 0.16	SG22	12–13.5	1	240
ZH ridge	SG36	5.5–6.5	5.435–6.33	5.40 ± 0.50	SG37, SG38	2.5–4	2.75	327, 44